Theor Chem Acc (2007) 118:305–314
DOI 10.1007/s00214-007-0261-2

REGULAR ARTICLE

Cationic dye dimers: a theoretical study

P. Homem-de-Mello · B. Mennucci · J. Tomasi · A. B. F. da Silva

Received: 22 June 2006 / Accepted: 2 January 2007 / Published online: 22 February 2007

Abstract In this work we present a quantum-mechanical study on the structure and electronic spectra of three cationic dyes monomers and dimers: acridine orange (AO), proflavine (PF) and methylene blue (MB). The geometries were obtained from crystallographic data, the electronic properties were calculated with DFT (B3LYP functional) and the theoretical spectra were obtained with ZINDO. The solvation methodology adopted was the Integral Equation Formalism (IEF) version of the Polarizable Continuum Model (PCM). This study shows that the differences, even small, between optimized and crystal geometries are responsible for important spectral characteristics. Also, it indicates possible structures for interacting dimers.

Keywords Cationic dyes dimer · ZINDO · IEF-PCM

1 Introduction

Methylene blue (MB), acridine orange (AO) and proflavine (PF) are cationic dyes and have been used as probes in the study of microheterogeneous and biological systems (clays, micelles, vesicles, microemulsions, DNA and nucleosides) due to their photophysical and photochemical properties which strongly depend on the nature of the surrounding environment [1–6].

The absorption spectra of these dyes in dilute solutions are characterized by a band at a longer wavelength. Increasing dye concentrations results in a gradual replacement of this band by a band at a shorter wavelength. This metachromatic behavior is attributed to the aggregation of dye molecules, due to the interaction between aromatic ring π electrons, forming sandwich (also called face-to-face) dimers [7,8].

For the dimers, the theory [8,9] predicts a splitting of the monomer band into two transitions, one at higher energy and the other at lower energy with respect to the monomer transition. The intensity ratio of the two bands depends on the relative orientations of the two monomers (and thus of the corresponding transition dipole moments) in the dimer. Because in these chromophores the transition moments lie in the plane of the aromatic ring system, the intensity ratio provides information about the orientation of the chromophores in the dimer. In the limit of exact parallel orientation of the two identical chromophores in the dimer, the low energy band is forbidden due to the presence of a centre of symmetry.

When the cationic dyes are placed in microheterogeneous systems, they present the same metachromatic behavior observed in pure aqueous solutions at higher concentrations. Polyelectrolytes and nucleic acids act as a pattern for the dye molecules, forcing them into a geometry that favors aggregation while clays facilitate the aggregation because the dye molecules are adsorbed on the surfaces, creating high-concentration regions. In the case of the adsorption on clay minerals, cationic dyes,

P. Homem-de-Mello (✉)
Centro de Ciências Naturais e Humanas,
Universidade Federal do ABC, Rua Santa Adélia,
166, CEP 09210-170 Santo André – SP, Brazil
e-mail: paula.mello@ufabc.edu.br

B. Mennucci · J. Tomasi
Dipartimento di Chimica e Chimica Industriale,
Università di Pisa, Via Risorgimento 35, 56126 Pisa, Italy

A. B. F. da Silva
Grupo de Química Quântica, Departamento de Química
e Física Molecular, Instituto de Química de São Carlos,
Universidade de São Paulo, C.P. 780, 13560-970
São Carlos – SP, Brazil

especially MB, are useful in determining the cation-exchange capacity, the surface area and differentiating kinds of clays in mixtures [8].

In a previous work [10] we have performed a quantum-mechanical study on the solvent effects in the structure and the electronic spectra of these cationic dyes using the Integral Equation Formalism (IEF) [12–14] version of the Polarizable Continuum Model (PCM) [15,16]. By using both time-dependent DFT (TDDFT) and ZINDO descriptions we have found that dyes belonging to the same family (for example, AO and PF belong to the acridine's family) present calculated absorption maxima closer than in the experimental spectra. In this work we present a further investigation of the previous results by studying dimeric structures extracted from the crystals of the same cationic dyes (MB, AO and PF) in order to verify if the aggregation effects observed in experimental studies when dye concentration is increased can explain the differences found between calculated and experimental spectra.

As discussed by Brocks [11], semiempirical methods are not very well suited to describe the weak intermolecular bonding of π-dimers, whereas ab initio Hartree–Fock calculations require the inclusion of correlation terms, what is not feasible for large systems. Following this analysis and the suggestion given in that paper, in this work, electronic properties are calculated by using the DFT method. In addition, as we have previously demonstrated [10] that the ZINDO method predicts the absorption spectrum for this kind of dyes rather well, calculations of the absorption spectra are also performed using ZINDO.

2 Computational methods

All calculations were performed with Gaussian03 code [36]. The general structure and the numbering scheme adopted for the monomers of the cationic dyes studied here are presented in Fig. 1.

MB is a thiazine family dye and AO and PF are acridine family dyes, that is, atom X corresponds to nitrogen for AO and PF and to sulfur for MB; and atom Y corresponds to carbon for AO and PF and to nitrogen for MB. Atoms 16, 17, 19 and 20 make the difference inside the families because are hydrogen for PF and methylic groups for AO and MB.

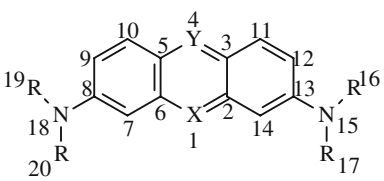

Fig. 1 General structure and the numbering scheme adopted for the monomers of cationic dyes studied

We have selected from Cambridge Database [17] two crystals for each cationic dye studied here. So, we have carried out a single point calculation for each monomer and dimer (see structures in Fig. 2) with the DFT method using the B3LYP functional [18–20] with the 6-31G(d) basis set. We have also performed ZINDO [21–27] calculations to obtain the absorption spectra and we have compared the results with experimental data. This methodology, as shown in a previous work [10], gives quite good results (errors about 5%) when compared to experimental data of these dyes.

The solvent (water) effect was always simulated in the calculations through the IEF-PCM method. The cavity in which the solute is embedded is obtained as a superposition of overlapping spheres centered on heavy atoms defined in terms of van der Waals radii [28] multiplied by 1.2 (only the hydrogen atoms bonded to nitrogen have their proper sphere). The radii are: 2.40 for $–CH_3$, 2.28 for –CH, 2.04 for –C, 1.92 for –N, 1.44 for H bonded to N and 2.16 for S.

3 Results and discussion

The unit cells found for the same dye in the Cambridge Database are different because of the counterion and/or the hydration. Namely, the crystals utilized were the following:

- MB: Mapaz (methylene blue chloride pentahydrate) [29] and Mbluet (methylene blue thiocyanate) [30];
- AO: Cesmao (acridine orange hydroiodide) and Cesmes (acridine orange hydrochloride monohydrate) [31];
- PF: Proflc (proflavine dichloride dehydrate) [32] and Proflv (proflavine monohydrate) [33].

In the previous study [10] we have presented the results for different cationic dyes, including the monomers of the dyes studied here. The geometries presented there, obtained by the optimization with B3LYP/6-31 +G(d)/ IEFPCM, are now compared to crystal monomer structures in Tables 1, 2 and 3. All the optimized structures are planar and the angles and bonds perfectly symmetric in relation to a line traced from atom 1 to atom 4 (see Fig. 1).

The crystal Mbluet monomer is planar as the MB optimized structure but its bonds are shorter. Mapaz is not planar, with the S atom region out of the plane, and the bonds are shorter as well.

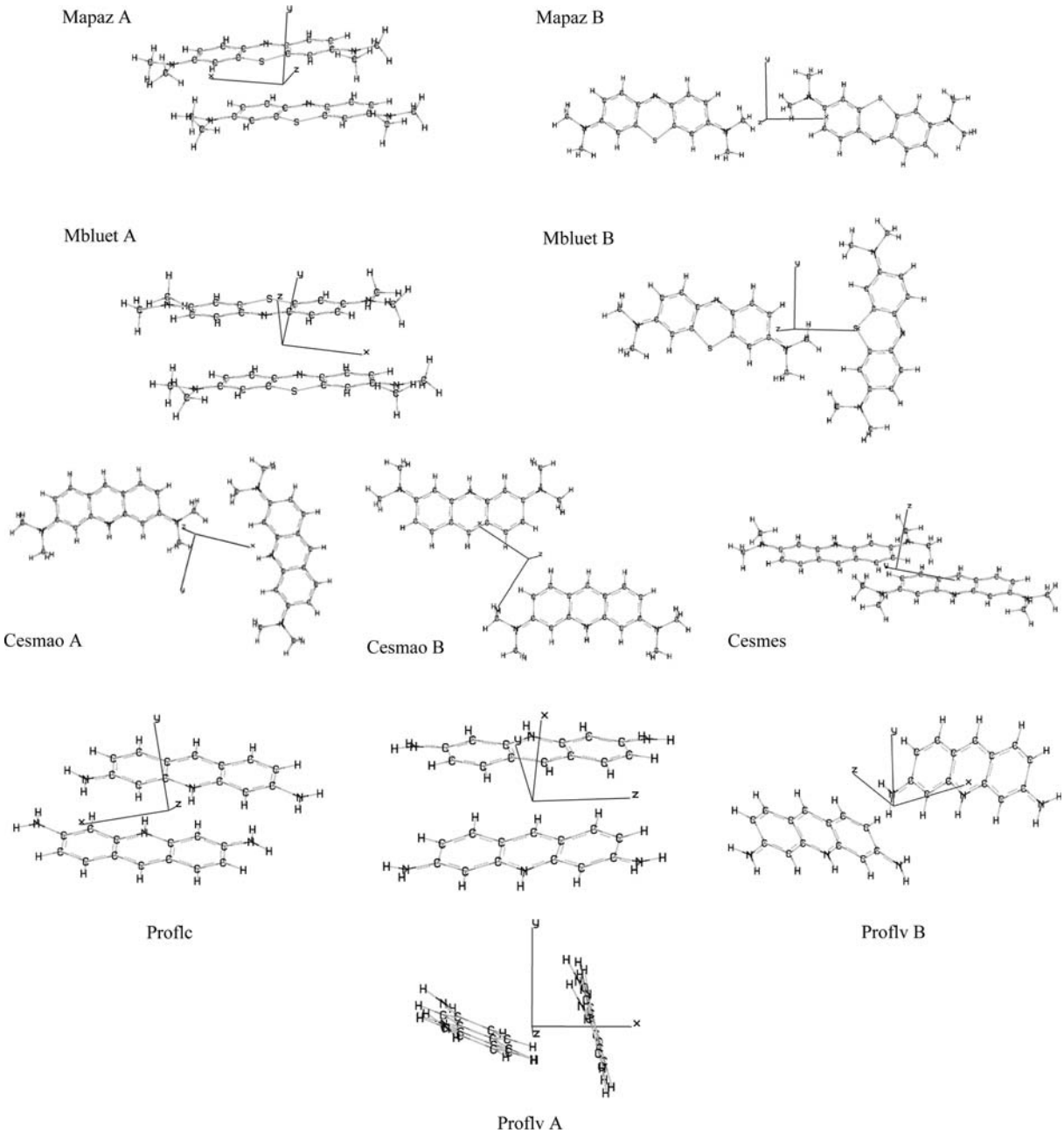

Fig. 2 Dimer structures extracted from crystals for MB (Mapaz and Mbluet), AO (cesmao and cesmes) and PF (Proflc and Proflv) with cartesian axes adopted

Both crystal monomers of AO are twisted, that is, a portion of atoms is above and the other one is under the plane of the central ring of the molecule: for example, C9, C10, N1 and C14 are above, C7 and C11 under and C4 in the plane. In Cesmes, one aliphatic group ($N(CH_3)_2$) is above and the other is under the plane, while in Cesmao, both aliphatic groups are under the plane.

Also PF crystal monomers are not planar. Proflc has an extremity ring with bonds shorter than the ones of the other extremity ring. Proflv is more symmetric than Proflc, but the central ring is folded so that the extremity rings and aliphatic atoms are above the plane.

In our previous work [10], we concluded that absorption spectra of these dyes consist in a charge transfer along the long-axis direction from the extremity atoms (those bonded to the extremity rings) to the atoms of the central ring of the molecules. Also for the monomers extracted from the crystals, the same behavior is observed but the differences in the structures cause changes in the excitation energies.

Table 1 Some structural parameters for each monomer studied here and obtained from MB crystals and optimization [10]

Torsion angle (deg) and bond length (Å)	Optimized structure	Mapaz	Mbluet
C6–C5–C10–C9	0.0074	−0.4861	0.0000
C6–C5–N4–C3	0.0019	−0.6182	0.0000
C2–C3–C11–C12	−0.0023	−0.7981	0.0000
C3–C2–S1–C6	−0.0131	1.3118	0.0000
C11–C12–C13–N15	179.9850	178.7510	180.0000
C10–C9–C8–N18	179.9800	178.7880	180.0000
S1–C2	1.7506	1.7387	1.7430
C6–S1	1.7506	1.7209	1.7357
C3–N4	1.3371	1.3363	1.3290
N4–C5	1.3371	1.3374	1.3531
C7–C8	1.4236	1.4212	1.4015
C13–C14	1.4236	1.4018	1.3908
C8–C9	1.4405	1.4457	1.4462
C12–C13	1.4406	1.4231	1.4367
C10–C5	1.4319	1.4167	1.4081
C3–C11	1.4319	1.4209	1.4052
C13–N15	1.3518	1.3427	1.3467
C8–N18	1.3517	1.3303	1.3135

Table 2 Some structural parameters for each monomer studied here and obtained from AO crystals and optimization [10]

Torsion angle (deg) and bond length (Å)	Optimized structure	Cesmao	Cesmes
C6–C5–C10–C9	−0.0050	−2.0384	1.0379
C6–C5–C4–C3	−0.0014	−0.3239	−1.8726
C2–C3–C11–C12	0.0234	−1.7317	0.1739
C3–C2–N1–C6	0.0046	−1.1578	0.8813
C11–C12–C13–N15	179.9710	−179.3370	178.3250
C10–C9–C8–N18	179.9610	−179.7890	−177.5150
N1–C2	1.3742	1.3541	1.3605
C6–N1	1.3742	1.3670	1.3676
C3–C4	1.3985	1.3825	1.3864
C4–C5	1.3985	1.3777	1.3972
C7–C8	1.4127	1.3839	1.3900
C13–C14	1.4127	1.3998	1.3961
C8–C9	1.4433	1.4451	1.4434
C12–C13	1.4433	1.4496	1.4449
C10–C5	1.4260	1.4298	1.4095
C3–C11	1.4260	1.4241	1.4279
C13–N15	1.3604	1.3440	1.3609
C8–N18	1.3604	1.3604	1.3504

By comparing the absorption wavelengths obtained for the different dyes using the optimized geometry (MB = 651 nm, AO = 455 nm and PF = 442 nm [10]) and the geometry extracted from the crystal structures to the experimental data in solution (see Table 4), we can conclude that using crystal geometries for MB and AO does not lead to significant changes with respect to optimized structures (we only found a slightly better agreement with the experimental values), while for PF both crystal structures lead to a larger difference and a worse agreement with experiments with respect to the optimized structures.

As mentioned before, the experimental spectral behavior is different from theoretical results when we analyze the changes passing from one dye to the other. The difference in experimental absorption maxima for AO and PF is equal to 50 nm while theoretical calculations [10] give a difference of about 15 nm. In our previous work [10], we have attributed these differences to the presence (or absence) of $N(CH_3)_2$ groups in the aliphatic portion of the molecules which could be responsible for nonelectrostatic solute–solvent interactions not accounted for in our solvation model. In the case of monomers extracted from crystals, the difference between absorption maxima increases to about 30 nm, showing a better agreement with the experimental data. These results seem to suggest that the cationic dyes studied could be not planar in solution exactly as in the crystals.

Table 3 Some structural parameters for each monomer studied here and obtained from PF crystals and optimization [10]

Torsion angle (deg) and bond length (Å)	Optimized structure	Proflc	Proflv
C6–C5–C10–C9	0.0000	−0.1928	−5.5111
C6–C5–C4–C3	0.0000	−2.9603	−1.9995
C2–C3–C11–C12	0.0000	−0.1205	5.5168
C3–C2–N1–C6	0.0000	3.8945	−5.5057
C11–C12–C13–N15	180.0000	−176.6950	−170.6240
C10–C9–C8–N18	180.0000	−177.6460	170.6280
N1–C2	1.3731	1.3693	1.3348
C6–N1	1.3732	1.3933	1.3348
C3–C4	1.3983	1.3970	1.3995
C4–C5	1.3984	1.3782	1.3996
C7–C8	1.4037	1.4128	1.3810
C13–C14	1.4037	1.3572	1.3810
C8–C9	1.4372	1.4352	1.4540
C12–C13	1.4372	1.3906	1.4540
C10–C5	1.4282	1.4428	1.4019
C3–C11	1.4282	1.4336	1.4019
C13–N15	1.3553	1.4755	1.3637
C8–N18	1.3552	1.3274	1.3637

Table 4 ZINDO/IEFPCM absorption wavelengths (λ_{max} in nm) and the corresponding oscillator strengths (f) and transition dipole moments (μ_x in au) calculated for each monomer obtained from crystals

Crystal	λ_{max}	f	μ_x^a	λ_{max}(exp)
MB from Mapaz	659	1.27	5.26	655 [8,34]
MB from Mbluet	658	1.25	5.21	
AO from Cesmao	453	1.07	4.00	492 [7]
AO from Cesmes	457	1.07	4.02	
PF from Proflc	428	0.87	3.51	445 [35]
PF from Proflv	424	0.89	3.52	

Experimental energies in water solution are also reported

[a] The μ_x are the transition dipole moment contributions in x direction (xy is the molecular plane and x direction is perpendicular to a line between X and Y atoms in Fig. 1); the μ_y and μ_z (contributions in y and z directions) values were omitted because they were too small (less than 0.05)

Another test to verify if the crystal structures are representative for cationic dyes in solution is the calculation of the spectra of the dimers.

Figure 2 presents the structures found for the dimers. For MB, four dimer conformations are available: Mapaz A and B (from Mapaz crystal) and Mbluet A and B (from Mbluet crystal). Mapaz A and Mbluet A are sandwich dimers, both monomers are almost parallel (in the first case also parallel to the xy plane). Mapaz A presents an extremity ring of one monomer superposed to the central ring of the other one, and the distance between monomers (from the C6 of one monomer to the S of the other) is equal to 3.6 Å, while in Mbluet A one monomer is rotated 180°, the rings are almost superposed and the distance from N4 of one monomer to the C2 of the other one is equal to 3.5 Å.

Mapaz B and Mbluet B are co-planar dimers and the monomers are in the same plane (xy). In the first case, one monomer is rotated 180° in relation to the other and the regions that are nearer between monomers are the aliphatic groups (distance from C16 of one monomer to the C16 of the other is equal to 3.4 Å), and, in the latter case, one monomer is rotated 90° in relation to the other and the smallest distance between monomers (from the H bonded to C14 of one monomer to a methylic H) is equal to 3.4 Å.

For AO, three dimer conformations were found: Cesmao A and B, from Cesmao crystal, and one dimer from Cesmes crystal. Cesmao A and B are co-planar dimers and the monomers are in the xy plane. In the first case, one monomer is rotated 90° in relation to the other and the regions that are nearer between monomers are the aliphatic groups (distance from C16 of one monomer to the C17 of the other is equal to 3.5 Å), and, in the second case, one monomer is rotated 180° in relation to the other and the smallest distance between monomers (from the H bonded to C10 of one monomer to the H bonded to C9 of the other) is equal to 3.1 Å. Cesmes is a sandwich dimer (both monomers are almost parallel) one monomer is rotated 180°; one $N(CH_3)_2$ of one monomer is superposed to an extremity ring of the other one; the distance from N18 of one monomer to the C8 of the other is equal to 3.6 Å.

As for AO, also for PF three dimer conformations were found: Proflv A and B, extracted from Proflv crystal, and one dimer from Proflc crystal. Proflv A and B present conformations between sandwich and T-dimers, that is, the plane of one monomer is almost perpendicular to the plane of the other one. In the first case, C10, C4 and C11 of one monomer point to the rings of the other

Table 5 ZINDO/IEFPCM absorption wavelengths (λ_{max} in nm) and the corresponding oscillator strengths (f), transition dipole moment contributions[a] (μ_x,μ_y and μ_z in au) and molecular orbitals (H = HOMO and L = LUMO) for each dimer obtained from crystals

Dimer	λ_{max}	f	μ_x	μ_y	μ_z	Transition[b]	λ_{max}(exp) [1,2,6]
Mapaz A	777	0.01	−0.05	0.07	0.40	H-1 → L+1 (0.25) H → L (0.65)	655 (dilute solution)
	603	2.20	6.53	−0.94	0.11	H-1 → L+1 (0.29) H → L (0.63)	
Mapaz B	669	2.51	7.41	−0.70	0.14	H-1 → (0.45) L H-1 →L+1 (−0.19) H → L (0.20) H → L+1 (0.44)	
	739	0.00	−0.03	0.00	−0.01	H-1 → L+1 (0.35) H → L (0.60)	
Mbluet A	596	2.59	−7.05	−1.03	−0.23	H-1 → L (0.48) H → L+1 (0.49)	605 (concentrated solution)
Mbluet B	661	1.18	4.04	3.07	0.00	H-1 → L (0.42) H-1 → L+1 (−0.24) H → L (0.25) H → L+1 (0.44)	
	652	1.33	−3.33	4.17	0.00	H-1 → L (0.49) H → L+1 (−0.48)	
Cesmao A	456	1.22	3.95	1.65	0.07	H-1 → L (−0.47) H → L+1 (0.48)	492 (dilute solution)
	451	0.93	1.47	−3.42	−0.06	H-1 → L (0.49) H → L+1 (0.47)	
Cesmao B	453	2.13	4.78	2.98	0.14	H-1 → L+1 (−0.45) H → L (0.52)	470 (concentrated solution)
Cesmes	459	2.07	5.38	−1.16	0.99	H-1 → L (−0.25) H-1 → L+1 (−0.34) H → L (0.38) H → L+1 (−0.37)	
Proflc	464	0.00	−0.02	−0.01	0.00	H-1 → L+1 (0.28) H → L (0.62)	445 (dilute solution)
	418	1.47	−4.37	−1.07	0.11	H-1 → L (0.49) H → L+1 (0.47) H-1 → L (−0.44)	
	438	0.01	0.00	0.00	0.34	H-1 → L+1 (0.10) H → L (0.15) H → L+1 (0.49)	N.A (concentrated solution)
Proflv A	417	1.62	0.00	0.00	4.71	H-1 → L (0.45) H-1 → L+1 (−0.22) H → L (0.23) H → L+1 (0.38)	
Proflv B	426	1.69	−4.53	1.72	−0.45	H-1 → L (0.27) H-1 → L+1 (−0.35) H → L (0.51) H → L+1 (0.10)	

[a] Cartesian coordinates as presented in Fig. 2
[b] CI expansion coefficients for each excitation are in parenthesis

and the smallest distance between monomers is from the H bonded to C10 of a monomer and the C10 of the other that is equal to 2.7 Å . In Proflv B, the monomers are not exactly superposed and the smallest distance between monomers (from N15 of a monomer to the H bonded to C7 of the other) is equal to 2.9 Å. Proflc is almost a sandwich dimer (with monomers almost parallel to the xz plane); an extremity ring of one monomer is superposed to the central ring of the other, and the distance from N1 of one monomer to the C14 of the other is equal to 3.7 Å.

As said in the Introduction, experimental data seem to indicate formation of dimers in more concentrated solutions; we have thus used the dimeric structures to calculate the absorption spectra.

Table 5 presents the absorption wavelengths, oscillator strengths, transition dipole moments and the molecular orbitals involved in the main excited states calculated with ZINDO/IEFPCM for each dimer obtained from crystals. For all dimers, the molecular orbitals involved in the main transitions are HOMO-1, HOMO, LUMO

and LUMO+1 (see plot in Figs. 3, 4, 5). These molecular orbitals have atomic contributions similar to the monomers separately, that is, occupied orbitals (HOMO-1 and HOMO) are formed by atoms of the molecule extremities and virtual orbitals by atoms of the molecule center. However, the monomers contribute for molecular orbitals of the dimer in different ways, as we shall show below.

Mapaz A presents the characteristic splitting of the monomer transition with a forbidden transition at 777 nm (with $f = 0.0$) and an allowed band at 603 nm (with $f = 2.2$) in excellent agreement with the experimental values. As observed before for the monomers, the excitation mainly involves HOMO and LUMO for which both monomers contribute with a charge transfer in the longitudinal direction (the transition dipole moment contribution on x has the largest value) from the extremity atoms to the central ring of each monomer.

Mapaz B does not present the forbidden band and has a transition at 670 nm, which is larger than the absorption wavelength of the optimized monomer and very similar to the Mapaz crystal and experimental monomer values (see Table 5). Both HOMO-1 and LUMO are localized on just one monomer while HOMO and LUMO+1 are localized on the other monomer, so the corresponding transitions are characterized by a charge transfer in the longitudinal direction in each monomer. In contrast, the transitions HOMO-1 to LUMO+1 and HOMO to LUMO, with give smaller contributions, consist in a charge transfer from a monomer to the other (also in the x direction since this is a head-to-tail dimer).

Mbluet A has a spectrum similar to Mapaz A, but the absorption maxima are smaller. Mbluet B has two absorption maxima both close to the monomer absorption maximum. As observed for Mapaz B, also for Mbluet B the transitions correspond to individual excitations of the monomers, what is evidenced by the molecular orbitals involved and their contributions. For both excitations, the transition dipole moment has large contributions in x and y directions (corresponding mainly to the excitations of the monomers that are oriented in these directions). The second transition occurs at the same wavelength of the optimized monomer, since the crystal structure is similar to the optimized molecule. The first transition occurs at larger wavelength, probably because of the not negligible contributions of charge transfers between monomers.

Cesmao A has the same behavior as Mbluet B, but in this case the first excited state occurs at the same wavelength of the optimized monomer and there are no excitations in which occur a charge transfer from one monomer to the other. Cesmao B, as Mapaz B, does not present the forbidden band and has a transition at 453 nm, which is similar to the optimized monomer value. HOMO-1 and LUMO+1 have contributions on just one monomer and HOMO and LUMO on the other one, so the main transitions correspond to a charge transfer in the longitudinal direction in each monomer. As Cesmao B, Cesmes does not present the forbidden band and presents one excited state at 459 nm, but in this case the transitions from one monomer to the other (HOMO-1 to LUMO+1 and HOMO to LUMO) are very important (see CI coefficients in Table 6).

Proflc presents the behavior proposed in literature [8], with a forbidden transition (at 464 nm with $f = 0.0$) and a band with higher energy (418 nm with $f = 1.5$) than that of the monomer transition. The second excited state involves transitions from HOMO to LUMO+1 and HOMO-1 to LUMO and so both monomers contribute (with a charge transfer in the longitudinal direction) from the extremity atoms to the atoms of the central ring of each monomer.

The splitting is also observed to Proflv A: while the crystal monomer absorbs at 424 nm, the dimer presents a forbidden band at 438 nm and another one at 417 nm, with a charge transfer from one monomer to the other characterized by the HOMO-1 to LUMO and the HOMO to LUMO+1 transitions. Proflv B presents one important transition that is similar to the monomer transition. It is interesting to note that the occupied molecular orbitals of Proflv B have contributions from both monomers, while virtual orbitals have contributions only from one monomer; this seems to indicate charge localization when excitation occurs.

This analysis on the comparison of experimental spectra and the calculations on solvated monomer and dimers to verify the possibility of the existence of the dimeric structures in solution can be further developed by considering interaction energies. We have thus carried out a single point calculation for each monomer and dimer with the DFT method to compare their energies and verify if there is an attractive force between monomers to form the dimer (the results are presented in Table 6).

The large and positive energy differences indicate strong repulsive interactions between all the pairs of monomers especially for Mapaz. This fact seems to indicate instability of the dimeric structures when extracted from the crystalline environment. In order to verify if this instability is due to intermolecular distances which are not optimal for the solvated systems, we have repeated the same calculations for the least unstable dimers of each family (Mbluet B, Cesmao A, and Proflv B) by changing such a distance. We have analyzed a 2.0 Å

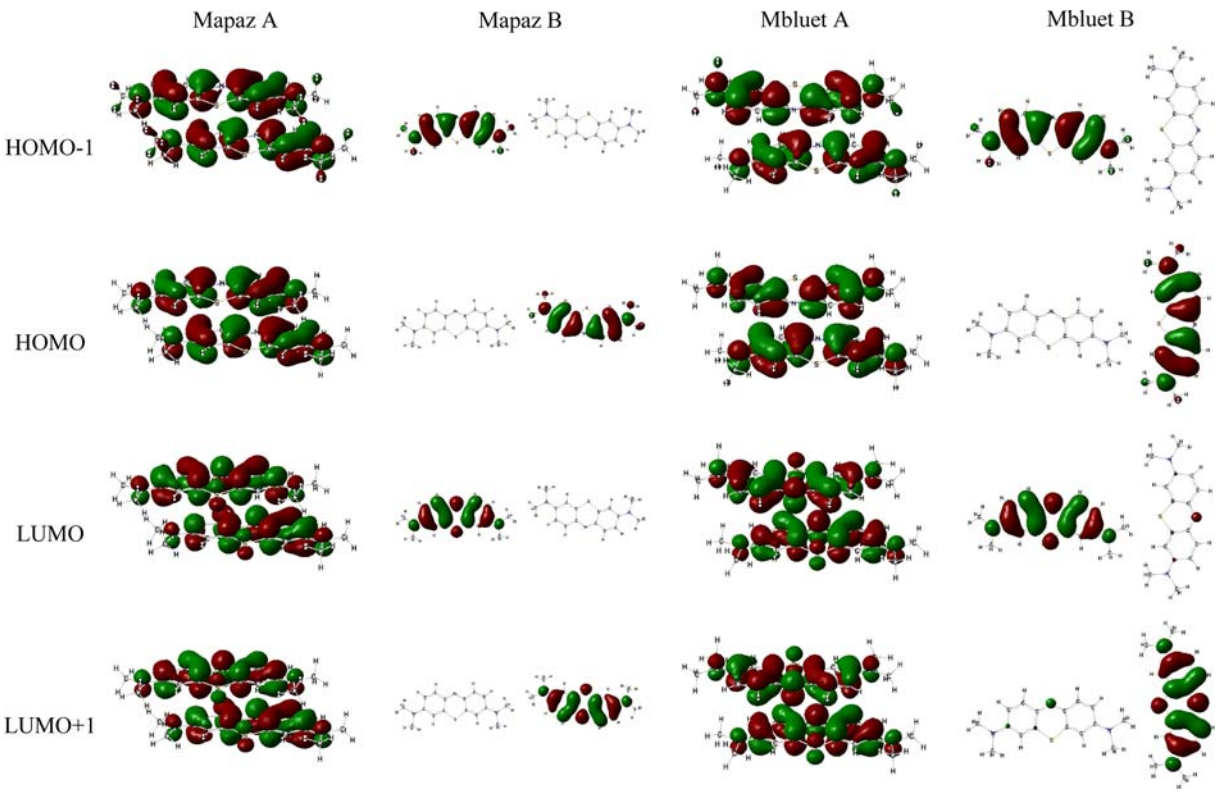

Fig. 3 Graphical representation of frontier molecular orbitals for MB's dimer structures

Fig. 4 Graphical representation of frontier molecular orbitals for AO's dimer structures

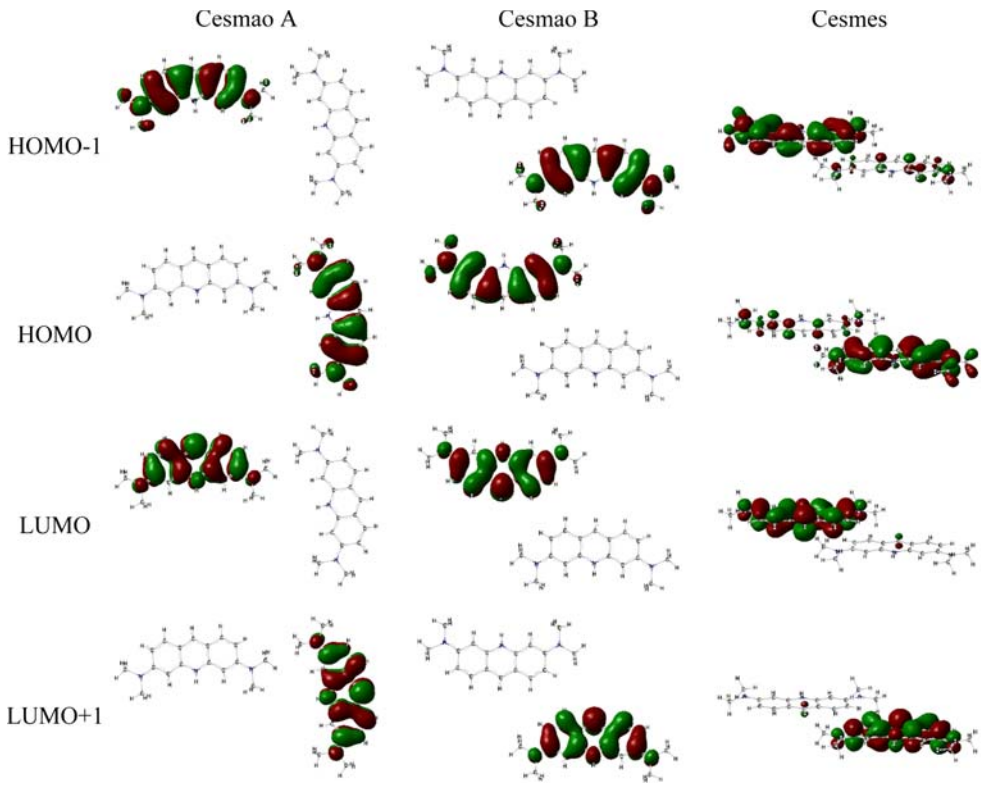

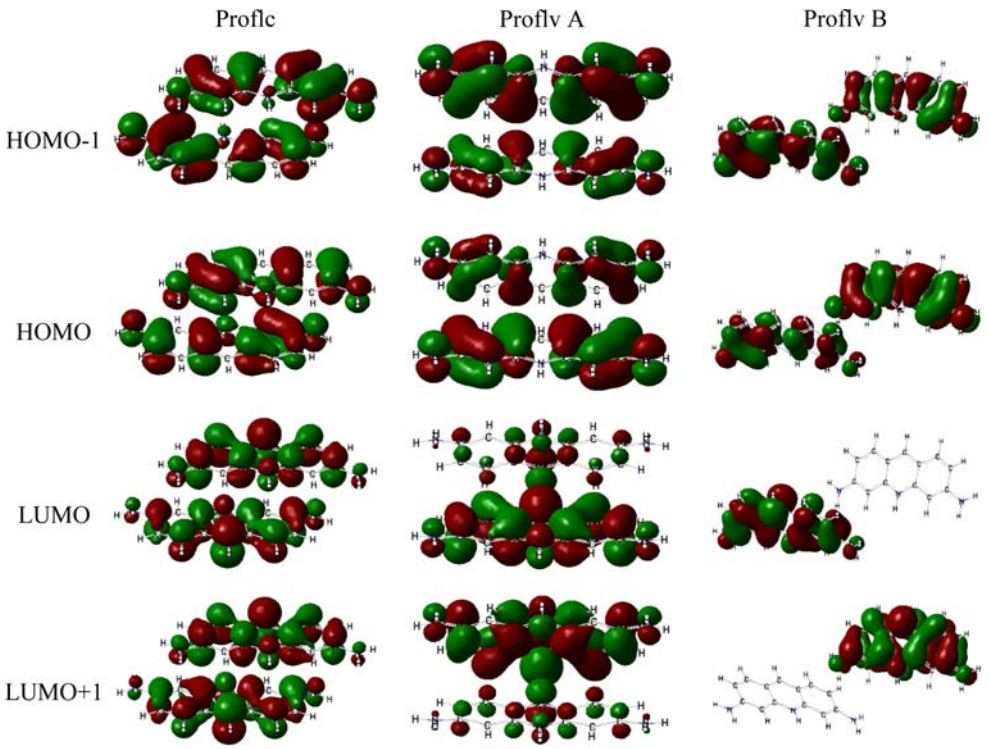

Fig. 5 Graphical representation of frontier molecular orbitals for PF's dimer structures

Table 6 Interaction energies calculated with B3LYP/6-31G(d)/IEFPCM for each dimer obtained from the crystal structures

Crystal	Dimer	$E_{T,Dim} - 2(E_{T,Mon})$
Mapaz	A	53.9
	B	43.9
Mbluet	A	5.6
	B	4.4
Cesmao	A	1.9
	B	1.9
Cesmes	–	3.8
Proflc	–	5.0
Proflv	A	3.8
	B	0.6

The energies expressed as $(E_{T,Dim} - 2E_{T,Mon})$ are in kcal mol^{-1}

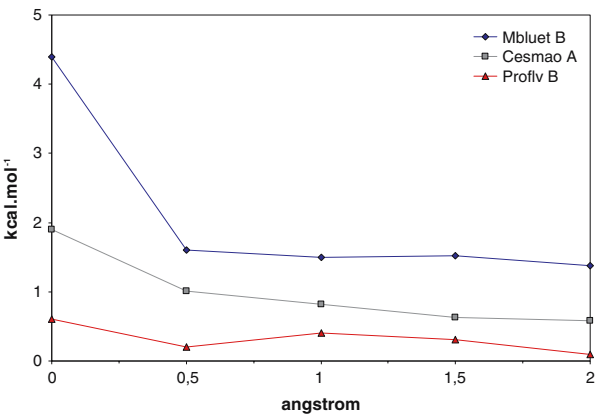

Fig. 6 Variation of the interaction energy for the least unstable dimers of each family (Mbluet B, Cesmao A, and Proflv B) as a function of the distance between monomers (the 0 corresponds to the crystal distance)

window of distances centered on the crystal intermolecular distance, in four steps of 0.5 Å. By decreasing the distance, the energies largely increase showing strong repulsive interactions; for this reasons in the Fig. 6 we report only the values obtained by increasing the distance.

As it can be seen from the figure, by increasing the distance between monomers from the crystal value a decrease of the interaction energy is found even if, for all molecules, the values remain positive.

4 Conclusions

In this work we have presented a quantum-mechanical study on the structure and electronic spectra of three cationic dyes in water solution: acridine orange (AO), proflavine (PF) and methylene blue (MB).

QM optimized geometries and geometries extracted from the crystal structure have been used and compared.

The main geometrical differences observed occur in the extremity rings and in the aliphatic regions making crystals less symmetric than the optimized structures. With exception of Mbluet, all monomers are not planar. The absorption spectra calculated for crystal monomers agree well with experimental data (mainly when comparing the family members) indicating that the interactions with the environment (another monomer or microheterogeneous systems) force them into a different geometry, even twisting the rigid structure formed by the three rings.

In order to verify if aggregation effects can explain the differences found between calculated and experimental spectra dimeric structures extracted from the crystals of the same cationic dyes have been also tested.

Analyzing the crystal unit cells, we have proposed four conformations for MB dimers (two sandwich and two coplanar dimers), three for AO (one sandwich and two coplanar dimers) and three for PF (none coplanar). We have analyzed the variation of interaction energy as function of the monomers distance.

For all the dimers studied, the molecular orbitals involved in the main transitions are HOMO-1, HOMO, LUMO and LUMO+1. Only Mapaz A, Mbluet A, Proflc and Proflv A, all sandwich dimers, could be considered as interacting dimers because they present a splitting in their spectrum (with relation to the monomer spectrum). By contrast, Mapaz B, Mbluet B, Cesmao A and B, all coplanar dimers, could not be classified as "normal" dimers, since their spectra correspond to the monomers ones, even if there is an influence of one monomer over the other. Cesmes and Proflv B are not coplanar or sandwich dimers and the aliphatic portions of the monomers are almost superimposed. In the latter case, the absorption spectra correspond to a charge transfer from one monomer to the other.

Acknowledgments The authors thank FAPESP, CAPES and CNPq (Brazilian agencies) for the financial support and one of us (PHM) thanks FAPESP and CAPES for the scholarships granted.

References

1. Neumann MG, Tiera MJ (1993) Química Nova 16(4):280
2. Neumann MG, Gessner F, Cione APP, Sartori RA, Schimitt CC (2000) Química Nova 23(6):818
3. Tatikolov AS, Costa SMB (2004) Biophys Chem 107:33
4. Choudhury M, Basu R (1995) J Photochem Photobiol A Chem 85:89
5. Gessner F, Schimitt CC, Neumann MG (1994) Langmuir 10:3749
6. Cione APP, Neumann MG, Gessner F (1998) J Colloid Int Sci 198:106
7. Cohen R, Yariv S (1984) J Chem Soc Faraday Trans 1 80:1705
8. Cenens J, Schoonheydt RA (1988) Clays Clay Miner 36:214
9. Cantor CR, Schimmel, PR (1981) Biophysical chemistry, Part II. Freeman, San Francisco, 846 pp
10. Homem-de-Mello P, Mennucci B, Tomasi J, da Silva ABF (2005) Theor Chem Acc 113:274
11. Brocks G (2000) J Chem Phys 112:5353
12. Cancès E, Mennucci B, Tomasi J (1997) J Chem Phys 107:3032
13. Mennucci B, Cancès E, Tomasi J (1997) J Phys Chem B 101:10506
14. Cancès E, Mennucci B (1998) J Math Chem 23:309
15. Miertus S, Scrocco E, Tomasi J (1981) Chem Phys 55:117
16. Cammi R, Tomasi J (1995) J Comp Chem 16:1449
17. Allen FH (2002) Acta Crystallogr B 58:380
18. Lee C, Yang W, Parr RG (1988) Phys Rev B 37:785
19. Miehlich B, Savin A, Stoll H, Preuss H (1989) Chem Phys Lett 157:200
20. Becke AD (1993) J Chem Phys 98:5648
21. Zerner MC, Lowe GH, Kirchner RF, Mueller-Westerhoff UT (1980) J Am Chem Soc 102:589
22. Anderson WP, Edwards WD, Zerner MC (1986) Inorg Chem 25:2728
23. Bacon AD, Zerner MC (1979) Theo Chim Acta 53:21
24. Ridley JE, Zerner MC (1976) Theo Chim Acta 42:223
25. Thompson MA, Zerner MC (1991) J Am Chem Soc 113:8210
26. Zerner MC, Correa de Mello P, Hehenberger M (1982) Int J Quant Chem 21:251
27. Hanson LK, Fajer J, Thompson MA, Zerner MC (1987) J Am Chem Soc 109:4728
28. Bondi A (1964) J Phys Chem 68:441
29. Marr HE, Stewart JM; CHIU MF (1973) Acta Crystallogr B 29:847
30. Kahnhara A, Ballard RE, Norris EK (1973) Acta Crystallogr B 29:1124
31. Mattia CA, Mazzarella L, Vitagliano V, Puliti R (1984) J Crystallogr Spectrosc Res 14:71
32. Obendorf SK, Carrel HL, Glusker JP (1974) Acta Crystallogr B 30:1408
33. Achari A, Neidle S (1977) Acta Crystallogr B 33:3269
34. Bergmann K, O'Konski CT (1963) J Phys Chem 67:2169
35. Cenens J, Vliers DP, Schoonheydt RA, De Schryver FC (1987) In: Schultz LG, Van Olphen H, Mumpton FA (eds) Proceedings of the international clay conference, Denver, 1985. The Clay Minerals Society, pp 352–358
36. Frisch MJ, et al. (2003) Gaussian03, Revision B.04, Gaussian, Inc., Pittsburg PA